

## **Evaluation of wind-induced dynamics of high-rise buildings by means of modal approach**

\*Lorenzo Rosa<sup>1)</sup>, Gisella Tomasini<sup>1)</sup>, Alberto Zasso<sup>1)</sup> and Aly M. Aly<sup>2)</sup>

<sup>1)</sup>Politecnico di Milano, Department of Mechanical Engineering, Via La Masa 1, 20156 Milan, Italy. e-mail: [lorenzo.rosa@polimi.it](mailto:lorenzo.rosa@polimi.it), [gisella.tomasini@polimi.it](mailto:gisella.tomasini@polimi.it), [alberto.zasso@polimi.it](mailto:alberto.zasso@polimi.it)

<sup>2)</sup> Alan G Davenport Wind Engineering Group, The Boundary Layer Wind Tunnel Laboratory, The University of Western Ontario, London, ON N6A 5B9, Canada, [aalysaye@uwo.ca](mailto:aalysaye@uwo.ca)

### **ABSTRACT**

This work applies a numerical and experimental procedure for investigating the dynamic behavior of tall buildings subjected to multidirectional wind loads. The procedure provides a framework for the calculation of the dynamic response based on the combination of wind tunnel test results and modal information. The procedure is applied to two different tall buildings: a slender tower with section aspect ratio  $B/D=2.6$  and height aspect ratio  $H/D=9$ , and a residential tower with "epsilon" section. Wind tunnel tests were performed on 1:100 scale rigid models to provide the surface pressure data essential for the procedure proposed in this work. A numerical modal approach is then used to evaluate the full-scale dynamics of the building.

With the proposed methodology it is possible to evaluate the effects of each mode in the peak acceleration (i.e. torsional mode and second bending modes in the two directions).

The methodology can also be used to evaluate interference effects, making new wind tunnel tests including in the set-up all the other tall buildings in the vicinity to the tower studied. These effects are worth to be examined in the design stage since they can greatly modify the response.

### **1. INTRODUCTION**

The dynamic response of tall buildings for serviceability and comfort analyses is usually evaluated using numerical standard codes (Eurocode 1, 2005; American Society of Civil Engineers, 2003; Zhou et al., 1999a,b; Kareem, 1992, 1988). However, the responses calculated using the standard codes are generally restricted to the first two bending modes; little guidance are provided by the norms for the estimation of the critical cross-wind and torsional responses, which usually have the greatest effect on most of tall buildings serviceability and comfort (Gu and Quan, 2004, Tallin and Ellingwood, 1984). In fact, the influence of the higher modes on the higher derivative of the displacement, i.e. acceleration and jerk, is quite significant. The adoption of the

standards lead then to a general underestimation of of the dynamic response as a consequence of neglecting the higher modes of vibration (Huang and Chen, 2007).

The procedure applied in this work, based on wind tunnel experimental measurements associated with a multimodal numerical model, allows to account for the effects of higher modes and interference effects of other buildings in the vicinity, as well as the angle of attack. For these reasons, it represents a valid alternative to the standard approach to assess building dynamic response in building serviceability and comfort studies.

The high frequency pressure integration (HFPI) technique is applied to directly evaluate the generalized forces necessary for solving the equations of motion. Through the integration of the pressure data, evaluated from simultaneous multiple pressure measurements on the surface of the building test model by means of synchronous multi-pressure sensing system, and knowing the modal information (natural frequencies, modal masses and mode shapes), it is then possible to calculate directly the generalized forces, and so the response of the building in terms of peak accelerations at the top of the building, for any number of modes of vibration of the building (Aly et al., 2011c,b,a; Xie and A., 2005).

Finally, starting from wind tunnel tests performed with and without the modelisation in the set-up of all the other tall buildings in the vicinity to the tower studied, is possible to evaluate the interference effects. These effects are worth to be examined in the design stage since it can greatly modify the buildings response.

This procedure, which a complete description can be found in (Rosa et al., 2012), is applied to two tall buildings excited by multidirectional wind loads. One building (called in the following Tower-A) is an office slender tower 220m tall with rectangular section (section aspect ratio  $B/D=2.6$ , height aspect ratio  $H/D=9$ ). The other building (called in the following Tower-B) is a residential tower 138m tall with an "ypylon" section. Since this tower is residential, it is expected there will be different possible openings, also dominant ones. This condition may generate large internal pressures in strong wind conditions, therefore in the facade design it is necessary to consider not only the pressure acting on the external surfaces, but also the internal ones. In order to evaluate the internal pressure a box with a dominant wall opening, representative of a "typical room" of the tower, has been made on the top of building. These data were then used to calibrate a numerical model to calculate the net-pressure coefficients on the entire surface of the tower. These studies can be found in (Giappino et al., 2009). Both the buildings are going to be built in Milan, Italy.

## **2. WIND TUNNEL TESTS**

Wind tunnel tests were performed at the 1.5MW closed circuit wind tunnel at the Politecnico di Milano, Italy. The large dimensions of the boundary layer test section (4m high, 14m wide and 36m long) allowed a very large geometry scale  $\lambda_L = 1:100$  to be used while maintaining lower blockage effects. The model of the towers, constructed as a rigid model, were manufactured using carbon-fibre and alucobond (a light-weight composite material) to achieve considerable stiffness and structural frequencies while keeping the weight as low as possible to reduce any inertial effects.

The wind tunnel tests were carried out in turbulent flow, simulating the vertical velocity and turbulence profile expected at the construction site (Milan city center) using spires and roughness elements. The whole area of the existing surroundings was also placed on the 13m diameter turntable. In this way it was possible to investigate all the wind exposure angles (from 0° to 360° with a step of 10°) while keeping the orientation of all the test buildings relatively unchanged.

Figure 1 shows the towers orientation with respect to the wind directions. The same figure shows also the reference system, fixed to the model, adopted for the definition of the aerodynamic forces: the origin of the coordinate system is in the center of the building section at its ground level  $(x_0, y_0, z_0)=(0,0,0)$ .

### 2.1 Interference effects

Since other tall buildings are planned to be build in the vicinity of Tower-A, two different configurations of surroundings were used and the interference effects were evaluated. In the first configuration (configuration I) Tower-A was secured in the test section where only the influence of the existing buildings in the vicinity of the tower (within a radius of 500m) were considered. In the second configuration (configuration II) all the new architectural project (including two other tall buildings planned to be built close to the tower called Tower-C1 and Tower-C2) were reproduced.

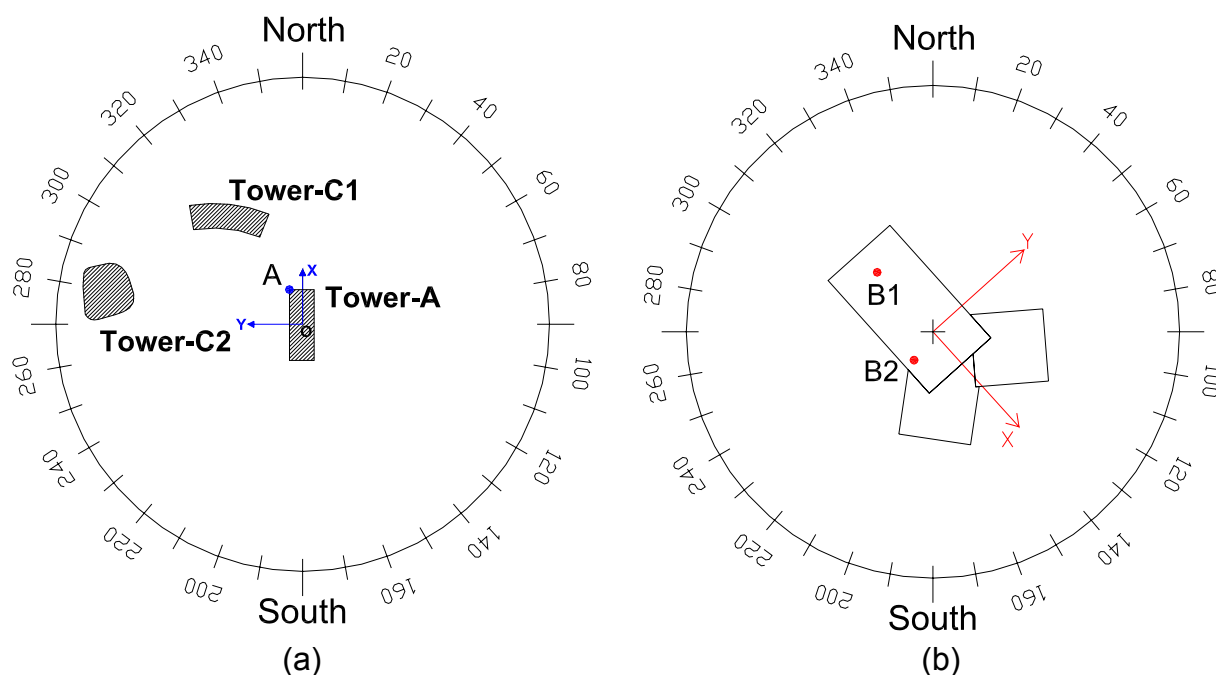


Figure 1. Towers orientation with respect to the wind directions and reference system for the calculation of the aerodynamic forces and top tower accelerations. (a) Tower-A, config. II. (b) Tower-B.

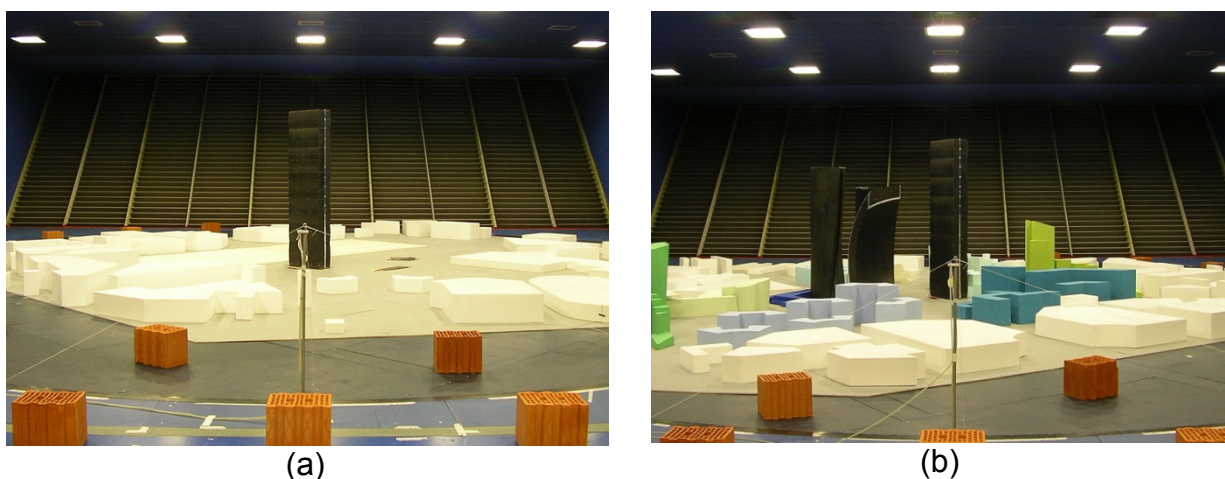


Figure 2. Tower-A, surroundings configurations tested in the wind tunnel: (a) Tower-A alone, config. I and (b) config. II, new whole complex on the turntable.

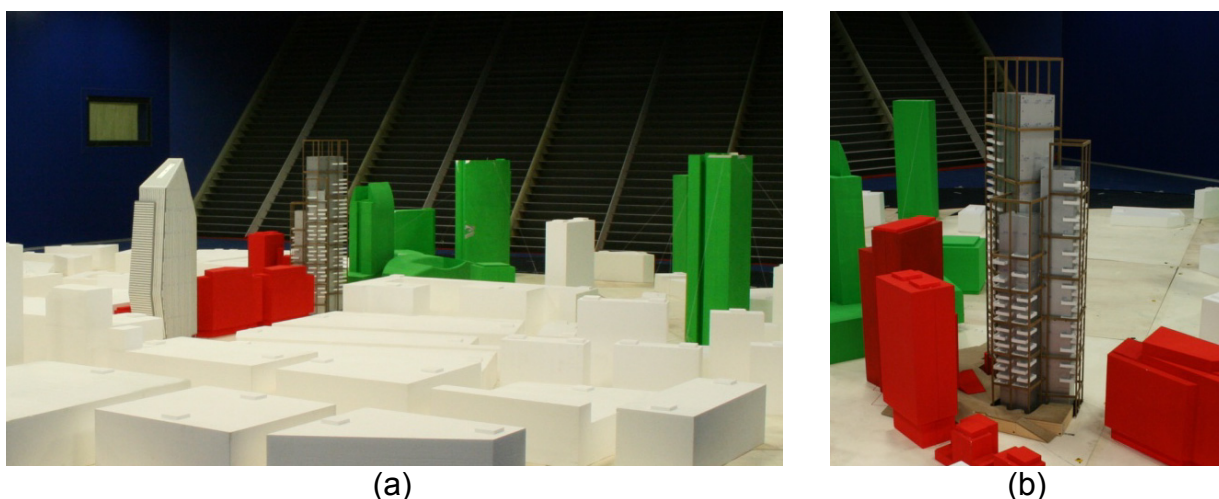


Figure 3. Tower-B in the boundary layer tests section. (a) View of the whole area. (b) Close-up of the tower studied.

### 2.1 Experimental set-up

The main objectives of the wind tunnel tests were the pressure measurements on the outer surface of the models. Pressure data were collected through high-frequency simultaneous measurements using 428 discrete points (pressure taps) on Tower-A and 224 pressure taps on Tower-B. The measurements were performed using the high-speed scanning pressure equipment PSI-system 8400 connected with electronic pressure scanners (ESP). The small dimensions of the scanners allowed them to be placed in the test model close to the measuring points, reducing the length of the tubes.

Pressures are presented as non-dimensional pressure coefficient  $C_{p,k}$  defined, at the  $k$ th pressure tap, as follows:

$$C_{p,k}(t) = \frac{p_k(t) - p_s}{\bar{q}_h} \quad (1)$$

where  $p_k(t)$  is the pressure time history at the  $k$ th pressure tap,  $p_s$  is the static reference pressure and  $q_H$  (Pa) is the dynamic pressure, evaluated considering the mean wind speed  $U_h$  at a reference height of  $h=100\text{m}$ .

### 3. THE MODAL APPROACH TO DYNAMIC ANALYSIS

#### 3.1. Evaluation of the dynamic response

The first step of the methodology is the calculation of the modal parameters, generally derived from a complete finite element model (FEM) of the building. In this study the first six mode shapes of the full-scale towers were used. The illustration of the modes with their natural frequencies are shown in Figure 4 for Tower-A and Figure 5 for Tower-B. The frequencies obtained from the FEM are shown in Table 1.

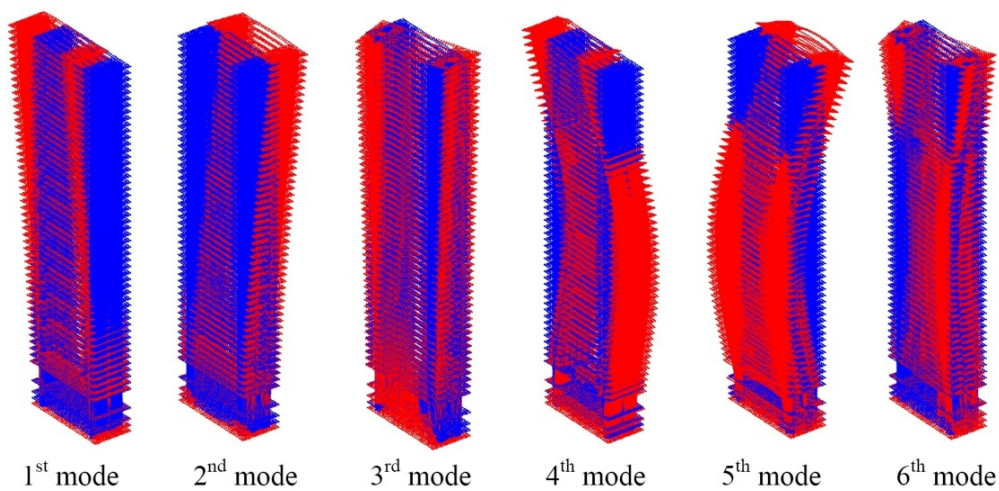


Figure 4. Tower-A, the first six mode shapes of the tower.

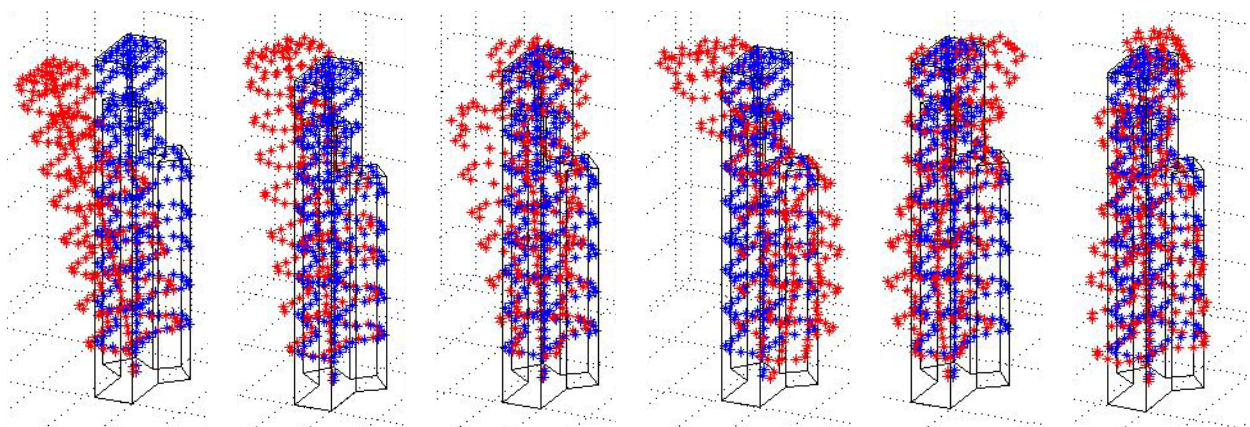


Figure 5. Tower-B, the first six mode shapes of the tower.

	f1 (Hz)	f2 (Hz)	f3 (Hz)	f4 (Hz)	f5 (Hz)	f6 (Hz)
Tower-A	0.144	0.153	0.254	0.451	0.627	0.881
Tower-B	0.20	0.21	0.30	0.71	0.81	0.89

Table 1. FE model frequencies: Tower-A and Tower-B.

In this paper the basic formulation of the method is presented. For a more complete description refer to (Rosa et al., 2012). The equation of motion governing the behavior of the structure, is:

$$\mathbf{M}\ddot{\mathbf{x}} + \mathbf{C}\dot{\mathbf{x}} + \mathbf{K}\mathbf{x} = \mathbf{F} \quad (2)$$

where  $\mathbf{x} = [x_1, x_2, \dots, x_{n-1}, x_n, y_1, y_2, \dots, y_{n-1}, y_n, z_1, z_2, \dots, z_{n-1}, z_n]^T$  is the  $(3n \times 1)$  displacement response vector ( $n$  is the number of the FEM nodes) and  $x_h, y_h$  and  $z_h$  are the  $h$ th nodal displacements along the  $x, y,$  and  $z$  axis, respectively.  $\mathbf{M}, \mathbf{C}, \mathbf{K}$  are respectively the mass, damping, and stiffness matrixes of the structure.  $\mathbf{F}$  is the time history vector of external forces acting at each  $h$ th node.

By applying a modal analysis approach (e.g. (Huang et al., 2010), (Tse et al., 2009)) and considering only the first six eigenmodes of the towers, the dynamic displacement response,  $\mathbf{x}$ , can be expressed in terms of modal contributions as follows:

$$\mathbf{x}(\mathbf{t}) = \mathbf{\Phi}\mathbf{q}(\mathbf{t}) \quad (3)$$

where  $\mathbf{q}(\mathbf{t}) = [q_1(t), q_2(t), \dots, q_6(t)]^T$  is the vector of the dimensionless generalized displacements and  $\mathbf{\Phi} = [\mathbf{\Phi}_1, \mathbf{\Phi}_2, \dots, \mathbf{\Phi}_6]$  is the eigenvectors matrix calculated from the FEM. In simple step the previous equation of motion can be written as:

$$\mathbf{M}_q \ddot{\mathbf{q}} + \mathbf{C}_q \dot{\mathbf{q}} + \mathbf{K}_q \mathbf{q} = \mathbf{Q} \quad (4)$$

where  $\mathbf{M}_q$  and  $\mathbf{K}_q$  are the mass and stiffness diagonal matrixes derived from the modal parameters of the structure (modal masses and natural frequencies),  $\mathbf{C}_q$  is the damping diagonal matrix and  $\mathbf{Q}$  is the lagrangian component of the external forces of the six considered modes. In this work the wind forces are the only external forces acting on the structure. Accordingly, considering the first six vibration modes, the lagrangian component of the forces of the wind for the  $i$ th mode is calculated as:

$$Q_{i,wind}(t) = \sum_{\nu} \sum_{k=1}^{N_{taps}} (p_k(t) \chi_k^{\nu} \phi_{i,k}^{\nu}) \quad i=1:6 \quad \text{and} \quad \nu = x, y, z \quad (5)$$

where  $p_k(t)$  is the pressure time history at the  $k$ th pressure tap,  $\chi_k$  is the associated tributary area (divided in the projections along  $x, y,$  and  $z$ ) and  $\phi_{i,k}^{\nu}$  is the value of the  $i$ th vibration mode along the  $\nu$ -axis at the position of the  $k$ th pressure tap. The analysis is effected, in the time domain, through step by step numerical integration of the equations of motion of the structure. The  $q_i(t)$  are then solved from each of the above equations. The response, in terms of displacements and accelerations of the real structure, can then be evaluated using equation (3).

#### 4. RESULTS

The simulations were carried out assuming a wind reference speed  $U = 28.5\text{m/s}$ , corresponding to a return period  $T = 10\text{years}$  and a structural damping, unless otherwise specified,  $\xi_S = 1\%$  for all of the modes. The value of the structural damping has been chosen in agreement with data collected from full-scale measures in Japan (Satake et al., 2003).

#### 4.1 Tower-A: top tower corner RMS accelerations

Figure 6 shows the rms accelerations of point A (Figure 1) in x-dir and y-dir for the tests in surrounding configuration I (Figure 3(a)) as a function of wind exposure  $\alpha$  and of the number of modes considered in the analysis. One can see the significant contribution of the torsional modes to the acceleration response. In particular, in x-dir acceleration is increased around at  $\alpha = 0^\circ$  and  $\alpha = 180^\circ$ , while in y-dir acceleration is greater at all exposure angles. This analysis shows the importance of considering the higher and the torsional modes in the evaluation of the maximum acceleration levels as their contribution is not negligible. A detailed analysis on this behavior, associated to the vortex shedding formation on a rectangular section, is reported in the already mentioned paper (Rosa et al. 2012).

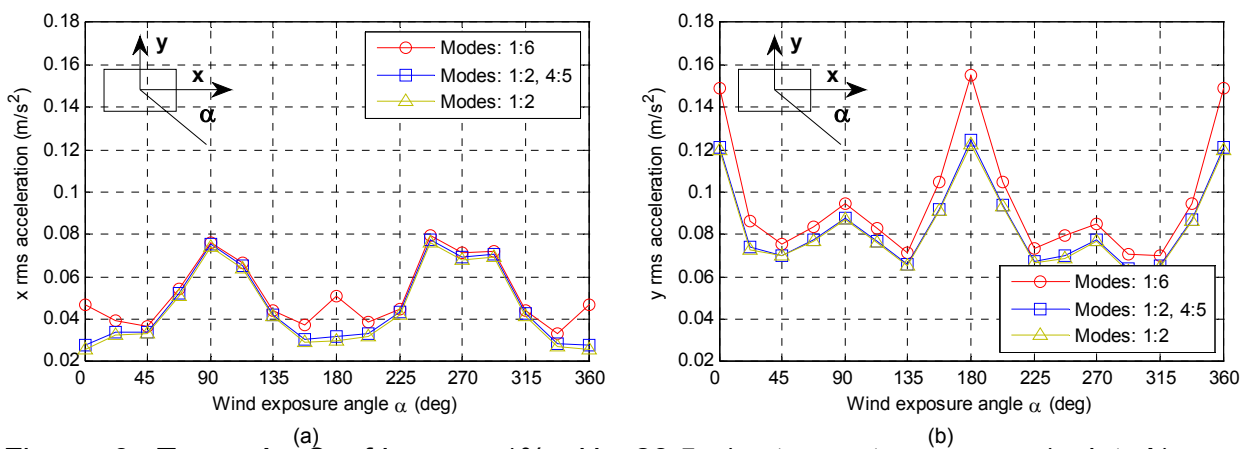


Figure 6. Tower-A. Conf.I,  $\xi_s = 1\%$ ,  $U = 28.5\text{m/s}$ , tower top corner (point A) rms acceleration as a function of  $\alpha$  and the considered modes: (a) x-dir, (b) y-dir.

#### 4.2 Tower-A: interferences effects

The proposed methodology is a valid tool to evaluate interference effects among adjacent structures. Using as input data the synchronous pressure measurements from the tests performed on the tower with the adjacent buildings (config.II, Figure 3(b)), it is possible to compute the lagrangian component of the external force (eq. (5)) taking into account possible effects due to the presence of other structures.

Figure 7 shows the comparison between configurations I and configuration II of the top tower corner (point A) rms displacements and accelerations in x-dir and y-dir. All the six modes were used in the analysis. Some significant changes in the response are present: in particular at  $\alpha = 180^\circ$  the presence of the adjacent tall buildings has a positive effect in both x-dir and y-dir, while at  $\alpha = 67.5^\circ$  the response in y-dir in config.II is higher.

In this example config.II is overall less critical than config.I; however the interference effects are worth to be examined in the design stage since they can greatly modify the buildings response, (Thepmongkorn et al., 2002).

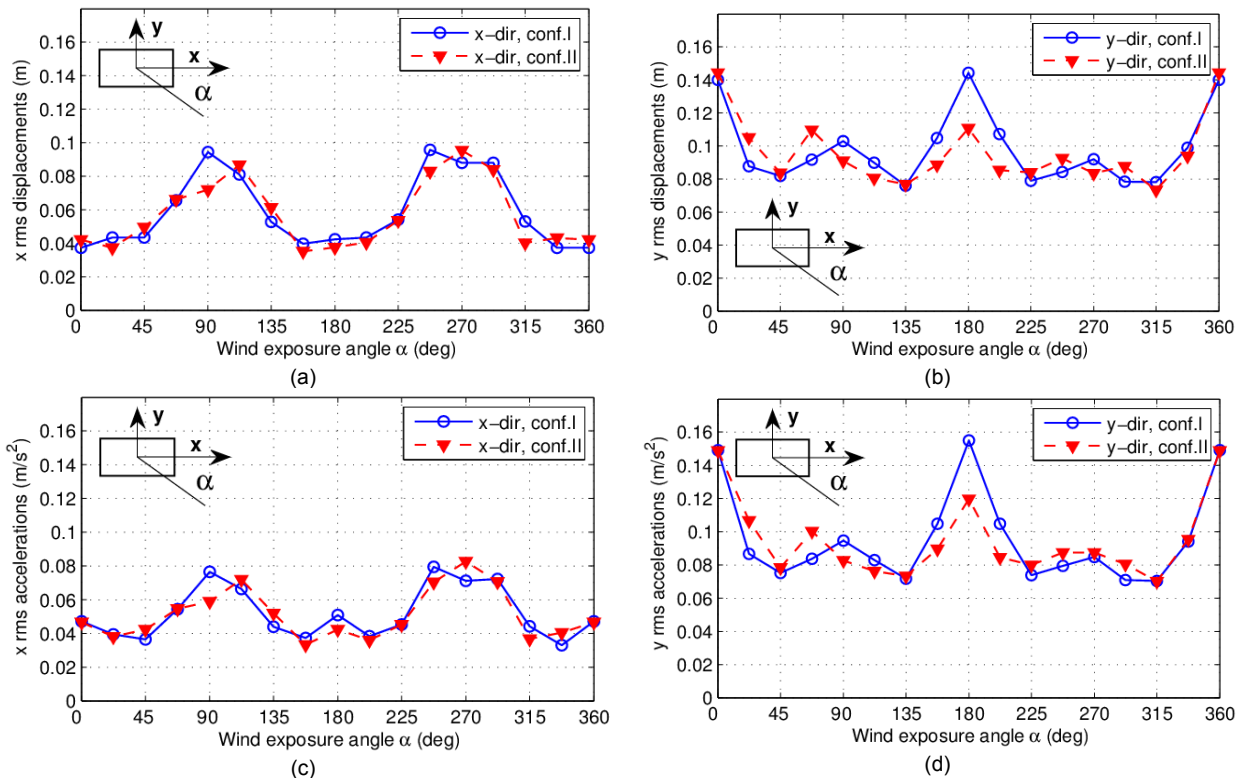


Figure 7. Tower-A. Rms of tower top corner (point A). Comparison between conf.I and conf.II.  $\xi_S=1\%$ ,  $U=28.5$  m/s, modes:1:6.

#### 4.3 Tower-A: evaluation of the peak acceleration

This methodology based on a modal approach allows also to estimate the maximum expected accelerations during the design stage as a function of different parameters: damping ratio, interference effects, modal shapes, etc. Figure 8 shows, for the configurations I and II, the top tower peak accelerations in x-dir and y-dir. The numerical simulations were carried out considering all six modes and assuming a structural damping  $\xi_S=1\%$ ,  $2\%$ ,  $4\%$  for all the modes. A 10year return wind speed (equal to  $U=28.5$  m/s) has been used to meet the client requests.

The figures show the effect of the increasing of the structural damping on the maximum acceleration response for both the configuration tested. In particular, it can be observed that, for the x-dir, to guarantee a maximum peak acceleration below the limit of 20milli-g (Kwok et al., 2009), a total damping  $\xi_S$  equal to 2% is sufficient, while, in y-dir, the total damping should be greater than 4%. This value could be reached both by increasing the structural damping, and by adding an external damping system, such as TMD or TLCDC (Diana et al., 2011).

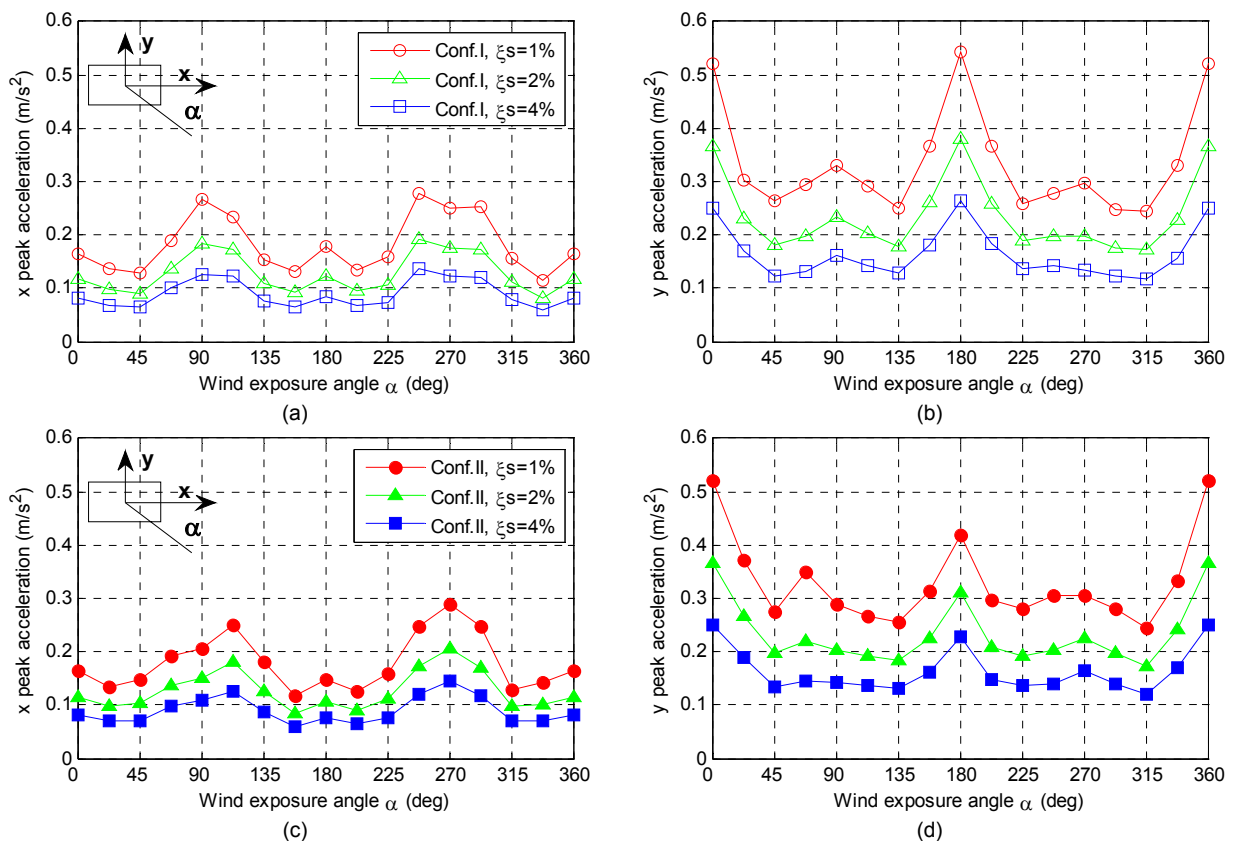


Figure 8. Tower-A. Peak acceleration of the tower top corner (point A). Comparison among damping ratio  $\xi_s=1\%$ ,  $2\%$ ,  $4\%$ .  $U=28.5\text{m/s}$ . (a) conf. I, x-dir. (b) conf. I, y-dir. (c) conf. II, x-dir. (d) conf. II, y-dir.

#### 4.4 Tower-B: evaluation of the peak acceleration

Figure 9 and Figure 10 show the peak accelerations of two points on the roof of Tower-B, respectively point B1 (center of the roof) and point B2 (on the border of the roof). The figures show the accelerations in x-dir and y-dir as a function of wind exposure  $\alpha$  and of the number of modes considered in the analysis. A structural damping  $\xi_s=1\%$  was used for all the simulations.

One can see the differences of the contribution of the higher modes to the acceleration response. In particular, in the central part roof (point B1, Figure 9) the first two modes are almost sufficient to calculated the total response. On the contrary closer to the border of the roof (point B2, Figure 10) the contributions of the higher modes is very important. Their maximum contribution occurs around the exposition angle  $\alpha=330^\circ$  in y-dir, when the part of the tower more similar to a rectangular prism is aligned to the wind direction. Figure 11 shows the spectra of the accelerations for this point at  $\alpha=330^\circ$ : one can see how the higher modes contributes to the total response, in particular in y-dir (Figure 11(b)) the third mode (first torsional) gives a contribution comparable to the first two fundamental modes.

The general behavior of Tower-B, compared with Tower-A, is less critical. The two buildings are very different since the "epsilon" shape of Tower-B gives more stiffness to the structure and a structural damping  $\xi_s=1\%$  is enough to obtain a peak accelerations lower than 20milli-g.

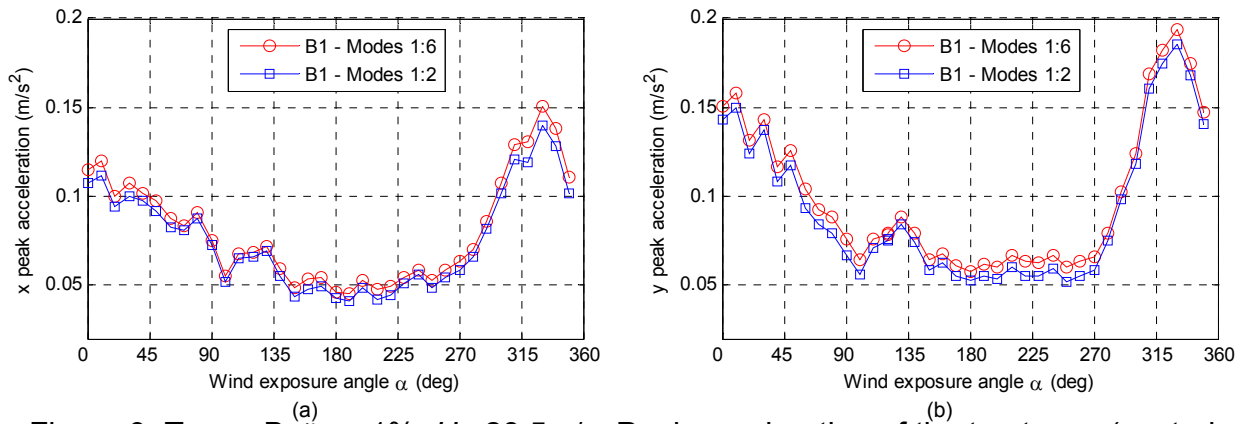


Figure 9. Tower-B.  $\xi_S = 1\%$ ,  $U = 28.5\text{m/s}$ . Peak acceleration of the top tower (central point B1) as a function of  $\alpha$  and the considered modes: (a) x-dir, (b) y-dir.

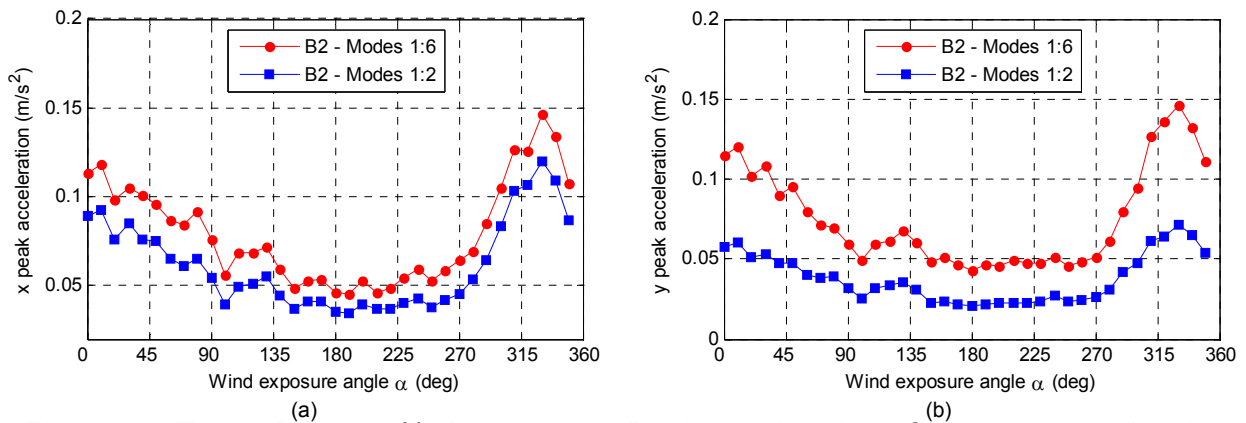


Figure 10. Tower-B.  $\xi_S = 1\%$ ,  $U = 28.5\text{m/s}$ . Peak acceleration of the top tower (border point B2) as a function of  $\alpha$  and the considered modes: (a) x-dir, (b) y-dir.

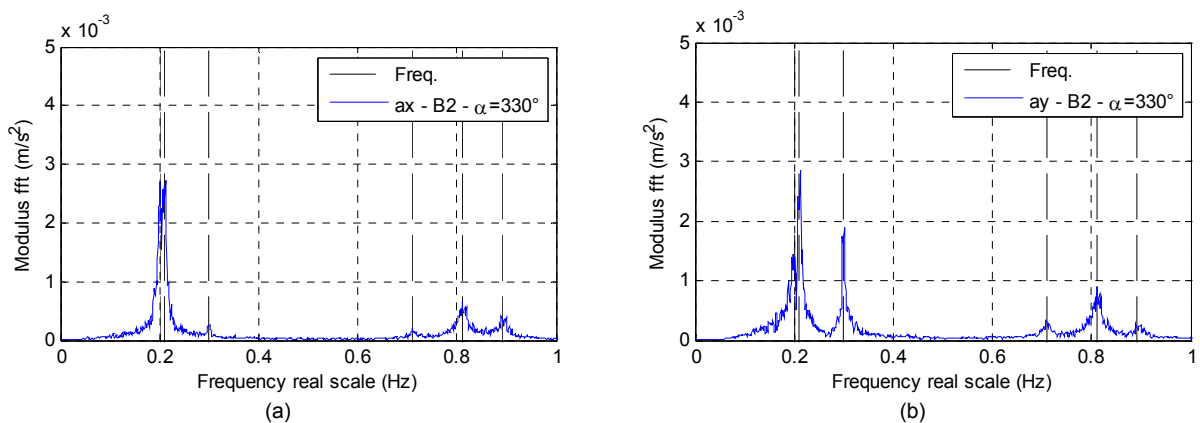


Figure 11. Tower-B.  $\xi_S = 1\%$ ,  $U = 28.5\text{m/s}$ . Spectra of the acceleration of the top tower (border point B2) at  $\alpha = 330^\circ$ . (a) x-dir, (b) y-dir.

## 5. CONCLUSIONS

This work applies a procedure for dynamic response prediction in high-rise buildings under wind loads. This numerical–experimental methodology requires, as input data, pressure distributions measured through wind tunnel tests on the external surface of the building as well as modal parameters of the full-scale structure. This allows us to evaluate the response of the building caused by turbulent wind. The procedure is applied to calculate the dynamic response of two high-rise building.

Results have shown that the response of the buildings in the cross-wind direction (lateral response combined simultaneously with torsion) can be higher than the response in the along-wind direction. This shows the importance of this methodology which has the advantage of combining lateral along-wind, lateral cross-wind, and torsional responses.

Using pressure distributions obtained from wind tunnel tests with different surroundings configuration it is easy possible to evaluate possible interference effects: e.g. it is possible to evaluate the effects of other tall building in the vicinity to the tower studied. These interference effects are worth to be examined in the design stage since they can greatly modify the buildings response.

The procedure can be used for the calculation of the response of the building in terms of maximum acceleration, useful to estimate the total amount of damping required to fulfill the comfort levels.

## REFERENCES

- Aly, A. M., Resta, F., Zasso, A., 2011a. Tall Buildings Under Multidirectional Winds: Response Prediction and Reduction, Wind Tunnels and Experimental Fluid Dynamics Research, dr. jorge colman lerner and dr. ulfilas boldes Edition.
- Aly, A. M., Zasso, A., Resta, F., 2011b. Dynamics and control of high-rise buildings under multidirectional wind loads. Smart Materials Research.
- Aly, A. M., Zasso, A., Resta, F., 2011c. On the dynamics of a very slender building under winds: Response reduction using mr dampers with lever mechanism. Struct. Des. Tall Spec. Build. Structural Design of Tall and Special Buildings 20 (5), 539–551.
- American Society of Civil Engineers, 2003. Minimum design loads for buildings and other structures. Reston, Va.
- Diana, G., Resta, F., Sabato, D., Tomasini, G., 2012. Experimental characterization and model of a modular square-section TLCD device. In: Proceedings of the 5th European Conference on Structural Control, EACS2012, Genoa, Italy.
- Eurocode 1, 2005. Actions on structures - Part 1-4: General actions - Wind actions. EN 1991-1-4.
- Giappino, S., Rosa, L., Tomasini, G. and Zasso, A., 2009. Internal pressure and façade loads on a residential tall building obtained from wind tunnel tests. WIT Transactions on the Built Environment, 105, pp. 287-297.
- Gu, M., Quan, Y., 2004. Across-wind loads of typical tall buildings. Journal of Wind Engineering and Industrial Aerodynamics 92 (13), 1147–1165
- Kareem, A., 1988. Aerodynamic response of structures with parametric uncertainties. Structural Safety 5 (3), 205–225.
- Huang, M. F., Tse, K. T., Chan, C. M., Kwok, K. C. S., Hitchcock, P. A., Lou, W. J., Li, G., 2010. An integrated design technique of advanced linear-mode-shape method and

- serviceability drift optimization for tall buildings with lateral-torsional modes. *Engineering Structures* 32 (8), 2146–2156.
- Huang, G., Chen, X., 2007. Wind load effects and equivalent static wind loads of tall buildings based on synchronous pressure measurements. *Engineering Structures* 29 (10), 2641–2653.
- Kareem, A., 1992. Dynamic response of high-rise buildings to stochastic wind loads. *Journal of Wind Engineering and Industrial Aerodynamics* 42 (1-3), 1101–1112.
- Kwok, K.C.S., Hitchcock, P.A., Burton, M.D., 2009. Perception of vibration and occupant comfort in wind-excited tall buildings. *Journal of Wind Engineering and Industrial Aerodynamics* 97 (7–8), 368–380.
- Rosa, L., Tomasini, G., Zasso, A. and Aly, A. M., 2012. Wind-induced dynamics and loads in a prismatic slender building: A modal approach based on unsteady pressure measurements, *Journal of Wind Engineering and Industrial Aerodynamics*, 107-108, pp. 118-130.
- Satake, N., Suda, K.-I., Arakawa, T., Sasaki, A., Tamura, Y., 2003. Damping evaluation using full-scale data of buildings in japan. *Journal of Structural Engineering* 129 (4), 470–477.
- Tallin, A., Ellingwood, B., 1984. Serviceability limit states: wind induced vibrations. *Journal of Structural Engineering* 110 (10), 2424–2437.
- Thepmongkorn, S., Wood, G. S., Kwok, K. C. S., 2002. Interference effects on wind-induced coupled motion of a tall building. *Journal of Wind Engineering and Industrial Aerodynamics* 90 (12-15), 1807–1815.
- Tse, K. T., Hitchcock, P. A., Kwok, K. C. S., 2009. Mode shape linearization for hfb analysis of wind-excited complex tall buildings. *Engineering Structures* 31 (3), 675–685.
- Xie, J., A., T., 2005. Design-oriented wind engineering studies for cctv new building. In: *Proceedings of the Sixth Asia-Pacific Conference on Wind Engineering*. Seoul, Korea.
- Zhou, Y., Gu, M., Xiang, H., 1999a. Alongwind static equivalent wind loads and responses of tall buildings. part i: Unfavorable distributions of static equivalent wind loads. *Journal of Wind Engineering and Industrial Aerodynamics* 79 (1-2), 135–150.
- Zhou, Y., Gu, M., Xiang, H., 1999b. Alongwind static equivalent wind loads and responses of tall buildings. part ii: Effects of mode shapes. *Journal of Wind Engineering and Industrial Aerodynamics* 79 (1-2), 151–158.